Infection and Drug Resistance

Dovepress
open access to scientific and medical research

Open Access Full Text Article

ORIGINAL RESEARCH

A Rapid PCR-Based Diagnostic Method for Skin Infection with *Mycobacterium marinum*

Yanan Li[1], Yahui Feng[2], Dongmei Li[3], Dongmei Shi[2,4], Guanzhi Chen[1]

[1]Department of Dermatology, Affiliated Hospital of Qingdao University, Qingdao, People's Republic of China; [2]The Laboratory of Medical Mycology, Jining No. 1 People's Hospital, Jining, Shandong, People's Republic of China; [3]Department of Microbiology & Immunology, Georgetown University Medical Center, Washington, DC, USA; [4]Department of Dermatology, Jining No.1 People's Hospital, Jining, Shandong, People's Republic of China

Correspondence: Guanzhi Chen, Department of Dermatology, Affiliated Hospital of Qingdao University, Qingdao, Shandong Province, 266000, People's Republic of China, Email chenguanzhiqd@hotmail.com

Objective: The increasing incidence of chronic skin infections caused by *Mycobacterium marinum*, coupled with the time-consuming and low detection rates nature of traditional culture and histological-based diagnostic methods, underscores the need for an expedited approach. The study aims to develop a rapid and efficient method for detecting *M. marinum* with PCR technology.

Methods: We designed four pairs of primers based on DNA sequences from GeneBank and prior studies, we utilized both PCR and Real-time PCR to identify *M. marinum*. Specificity and sensitivity assessments were conducted in vitro by DNAs extracted from *M. marinum* and other bacterial or fungal cultures. Further validation was performed through the implementation of a mouse skin infection model to optimize and confirm the efficacy of the detection method in both fresh and paraffin-embedded skin tissues. The same PCR testing system was further confirmed with paraffin-embedded skin tissues samples from patients as well.

Results: The results of the study indicate promising outcomes for the four-pair primers system. It demonstrated 100% sensitivity in detecting *M. marinum* from purified cultures, including typical strains and nine clinical isolates, while achieving a specificity of 100%. This specificity was evidenced by the absence of PCR products from 12 bacterial species, 12 fungi species, and six other non-tuberculous mycobacterium (NTM) species. In the animal model, the PCR assay exhibited high detection efficacy for both infected fresh tissues and paraffin-embedded tissues, with a slight superiority observed in fresh tissues. However, the PCR assay exhibited high detection efficacy for clinical paraffin-embedded tissues. These findings collectively underscore the robust detection capabilities of our four-pair primers in both in vitro and in vivo settings.

Conclusion: A sensitive and highly specific rapid detection system has been successfully developed that can be used to detect *M. marinum* in both infected fresh tissues and paraffin-embedded tissues.

Keywords: *Mycobacterium marinum*, bacteria, infected tissue, paraffin-embedded tissue, PCR technique

Introduction

Mycobacterium marinum, classified as a non-tuberculous mycobacterium (NTM) species, is commonly found in fresh or marine waters globally,[1] posing to health concerns for aquatic animals such as fish.[2–4] As an opportunistic pathogen, *M. marinum* can cause skin and soft tissue infection in human beings closely contact with fish and seawater such as fishermen, marine workers and swimmers.[5,6] The resulting skin lesions often manifest as granulomas, which are often described as "swimming pool granuloma" or "fish tank granuloma".[7] The clinical presentation of *M. marinum* shares similarities with *Sporothrix* and NTM infections. However, individuals with severely immunocompromised condition may experience deep-seated infections, including arthritis, osteomyelitis, and hematologic infections.[8,9] Despite the increasing incidence of *M. marinum* infections, accurate diagnose remains challenging based solely on clinical manifestations, often resulting in misdiagnosed with other pathogens.[10]

Clinical diagnosis of *M. marinum* infection currently rely on a comprehensive approach, incorporating medical history, skin manifestation, histologic and microbiologic examinations, and molecular identification methods.[11,12] In medical history, a crucial diagnostic clue lies in the patient's history of contact fish and aquatic exposure. Traditional

Received: 11 February 2024
Accepted: 29 June 2024
Published: 9 July 2024

culture methods for isolation and identification of *M. marinum* are still practiced in clinical settings. However, this method is inherently time-consuming, as this organism typically requires several weeks to form visible colonies on solid media. Additionally, the culture conditions and the quality of collected specimen are stringent factors contributing to the challenges associated with this approach.

Pathologically, the histologic features of *M. marinum* in the tissue closely resemble those of other mycobacterial infections, typically presenting with a lower abundance of acid-fast bacteria.[13] Currently, the challenge lies in the detection of low bacterial loads from both fresh or paraffin-embedded infected tissues. The advent of second-generation sequencing technology prompted the immediate application of this molecular diagnostic method in the clinical diagnosis of *M. marinum* infections, due to its high sensitivity and accuracy.[14] However, widespread adoption in clinical settings still faces obstacles due to some disadvantages such as high cost, a time-consuming approach, and difficulty in distinguishing from the normal microbiological flora of the skin. Therefore, there is an urgent need for a rapid and accurate diagnostic method for clinical setting.

In the realm of infectious agent diagnosis, molecular biology identification methods utilizing various PCR techniques have gained prominence, particularly in examining tissues. Like sequencing method, it is high sensitivity and relatively rapid diagnostic method. The application of these methods in clinical diagnostics for *M. marinum* infections dates back to 1996.[15,16] In this study, we employed 4- pair primer-PCR method to refine our diagnostic performance in vitro and assess diagnostic efficacy in an in vivo skin infection model.

Materials and Methods

DNA Extraction

A total of nine clinical strains of *M. marinum* were isolated and cultured from patients with *M. marinum* infection admitted to the First People's Hospital of Jining City from January 2021 to January 2022. Additionally, one type strain of *M. marinum* was included. Genomic DNA extraction from cultures of *M. marinum* and other bacteria involved the use of the FastPure Bacteria DNA Isolation Mini kit (Novozymes, China) after grinding bacterial mass for 1 minute. The grinding time extended to 3 minutes when preparing DNA from fresh mouse tissues, and the subsequent extraction was performed by using the FastPure Bacteria DNA Isolation Mini kit (Novozymes, China). DNA from paraffin-embedded tissues was extracted with the Paraffin Embedded Tissue DNA Extraction Kit (TIANGEN, China) following the manufacturer's instructions. The concentration and quality of extracted DNAs were assessed using a Nano spectrophotometer.

Design of Primers

Four pairs of *M. marinum*-specific primers were meticulously designed based on the gene sequences of 16S rRNA, rpoB, and hsp20 genes obtained from GeneBank. These primers, synthesized and prepared in Sangon Biotech (Shanghai, China), are outlined in Table 1 along with their respective sequences. Of these primers, the third and fourth pair primers

Table 1 Primers Used in the Study

Target Gene	Sequence	Annealing Temperature (°C)	Product Length (bp)
16S rRNA	F 5'CTTCGGGAT****CTGGGAAACTG 3'	60.2	353
	R 5'GCTTCTTCT****CTACCGTCAATC 3'	59.6	
rpoB	F 5'CAGCAGCC****GGTGGTAAG 3'	62	344
	R 5'CGAGACA****GATTCCGAGGTTG 3'	60.2	
Hsp20-1	F 5'CCGACCAG****AATGCCGATG 3'	61.4	272
	R 5'GCAGCTTC****CACCTTCCG 3'	62.3	
Hsp20-2	F 5'CGACCAGC****ATGCCGATG 3'	59.2	126
	R 5'GCGAACGG****CACATTGC 3'	60.5	

Notes: Diagnostic method, including the entire sequences of the primers shown here, is under a pending patent application with the China Patent Bureau.

were derived from conservative and variable area of hsp20 gene. To assess their specificity, the four primer pairs were subjected to electrophoretic gel analysis of amplification products, conducted without the addition of *M. marinum* DNA. This rigorous primer design process ensures the targeted and accurate amplification of *M. marinum* DNA in subsequent PCR analyses.

PCR and Real-Time PCR

For each 25 μL PCR reaction, 12.5 μL of 2× Accurate Taq Master Mix (dye plus), 0.5 μL of each upstream and downstream primer, and approximately 250 ng of template DNA were combined and replenished to 25 μL with RNase free water.

The PCR amplification was performed in a serial of steps: pre-denaturation at 94°C for 30 seconds, cycling for 25–35 times with denaturation at 98°C for 10 seconds, annealing at 57°C for 30 seconds, and extension at 72°C for 1 minute, and final extension at 72°C for 2 minutes. Subsequently, the PCR reaction products were detected by electrophoresis on 1.5% agarose gel and stained with ethidium bromide for visualization.

For Real-time PCR reaction, a total volume of 20 μL comprised 10 μL of 2× SYBR Green Pro Taq Hs Premix, 0.4 μL of each upstream and downstream primer, and DNA at indicated concentrations in each experiment. The conditions of Real-time PCR amplification were as follows: initial denaturation at 95 °C for 30s, followed by 40 cycles of denaturation at 95 °C for 5 s and annealing/extension at 60 °C for 30s.

Establishment of a Mouse Skin Infection Model

A mouse skin model of *M. marinum* infection was created using five quantitatively different inocula of *M. marinum* in eight-week-old female C57BL/6 mice. Following the shaving of a 1.5 cm×1.5 cm area on their backs, *M. marinum* was subcutaneously injected at varying concentrations: 3×10^8CFU, 3×10^7CFU, 3×10^6CFU, 3×10^5CFU, 3×10^4CFU of *M. marinum*. Typically, seven days after injection, redness and swelling of the skin on the back of the mice were observed, with significant swelling and gradually formation of superficial ulcers occurring within the subsequent 3–7 days. By 10–14 days post- infection, the mouse infection model had fully developed, and skin tissues from the infected sites were collected for pathological examination. A portion of the fresh tissues were prepared as paraffin-embedded tissues, while the remaining half served as the fresh tissue for subsequent experimental studies.

Evaluation of PCR and Real-Time PCR Performance in Fresh and Paraffin-Embedded Mouse Tissues Infected with M. Marinum

Each DNA preparation extracted from fresh skin samples underwent validation through both PCR and Real-time PCR analyses. The concentration of DNA in each preparation, used in both PCR methods, ranged from 1ng, 5ng, 10ng, 25ng, 50ng, to 100 ng against four pairs of primers, irrespective of their inoculated concentration. Notably, the Real-time PCR incorporated 1ng of DNA extracted from mouse tissue with minimal *M. marinum* injection.

The infected mouse skin was meticulously fixed and embedded in paraffin wax, subsequently sliced at a thickness of 10 μm, with 5–10 rolls per sample. The DNA preparation from each infected skin sample, including those obtained from sites with the lowest bacterial injection, was adjusted to a range of 1ng, 5ng, 10ng, 25ng, 50ng to 100 ng for both PCR reactions and the Real-time PCR reactions against four pairs of primers. This approach was intended to ensures a thorough assessment of the diagnostic efficacy across varying conditions of infected tissues.

Evaluation of PCR and Real-Time PCR Performance in Clinical Paraffin-Embedded Tissues Infected with M. Marinum

A total of four clinical skin tissue samples from patients with *M. marinum* infection underwent testing using our two PCR methods. These patients were admitted to the Department of Dermatology, First People's Hospital of Jining City in 2023. Biopsied skin tissue from clinical patients with suspected *M. marinum* infection were examined pathologically in paraffin-embedded tissues f.Each DNA preparation extracted from paraffin-embedded skin samples and subsequently validated through both PCR and Real-time PCR analyses, as described above. The concentration of DNA in each

preparation used in both PCR methods was standardized to 100 ng against four pairs of primers. This approach was intended to ensure a comprehensive assessment of the diagnostic efficacy for clinical skin samples.

Results

Evaluation of Sensitivity for Our Optimized 4-Pair Primers PCR System

We refined the primers used for diagnosis of *M. marinum*, deviating from the common practice of employing a single primer pair strategy for DNA evidence, as seen in most literature.The absence of dimer formation among 4-primer pairs (Figure 1A) validates the quality and specificity of these primers for subsequent experiments. Addition of typical strain *M. marinum* DNA, PCR product sizes for the 16S rRNA, rpoB, and hsp20 genes are 353 bp, 344 bp, 272 bp, and 126 bp, as visualized in lanes P1, P2, P3, and P4 of the electrophoretic images (Figure 1B).

The sensitivity of our 4-pair primer system was initially validated using 9 clinical *M. marinum* isolates that had been confirmed through sequencing in our prior study. Electrophoretic gel analysis revealed that PCR products from all 9 clinical *M. marinum* isolates migrated to the same positions as the target bands of the type strains in Figure 2A. PCR conducted with primer pairs 1 for 16S rRNA, 2 for rpoB, 3 for hsp20-1, and 4 for hsp20-2 genes showed identical sizes of PCR bands with typical strain DNA at concentrations of 100 ng, 10 ng, and 1 ng (**I-III**), as well as with 100 ng DNA from each clinical isolate in Figure 2A (IV-XII). Real-time PCR reaction displayed similar amplification curves between typical strain and clinical *M. marinum* strains for each primer pair (Figure 2B).

To further assess the sensitivity of our 4-primer pair system, varying amounts of *M. marinum* type strain DNA ranging from 10 ng to 0.01 ng were added to the PCR reactions. As shown in Figure 3A, electrophoresis Results following PCR amplification displayed the appearance of target bands at the expected locations for primer pairs 1 (sub-subfigure 3A I), 2 (sub-subfigure 3AII), 3 (sub-subfigure 3A III), and 4 (sub-subfigure 3A IV) across all tested DNA concentrations (10ng, 1ng, 0.08 ng, 0.06ng, 0.04 ng, 0.02ng, to 0.01ng). Moreover, distinct amplification curves for each primer pairs were observed across all seven tested concentrations of typical strains using the Real-time PCR system (Figure 3B).

Both PCR and Real-time PCR experiments affirmed a 100% sensitivity of our 4-primer pair system, at least within the 10–100 ng DNA concentration range. It is noteworthy that while the minimal detection limit for all primer sets was shown as 0.01 ng in Figure 3A, primer pairs for 16S rRNA and rpoB yielded more products.

Assessing the Specificity of Our 4-Primer Pairs System

To validate the specificity of our 4-primer pairs system, we meticulously selected twelve bacterial and twelve fungal species commonly prone to confusion with *M. marinum* in clinical diagnosis. The selected bacterial species were *Klebsiella pneumoniae, Staphylococcus aureus, Proteus mirabilis, Corynebacterium acetonicum, Escherichia coli, Enterococcus faecalis, Streptococcus anginosus, Staphylococcus epidermidis, Streptococcus hemolyticus, Morganella*

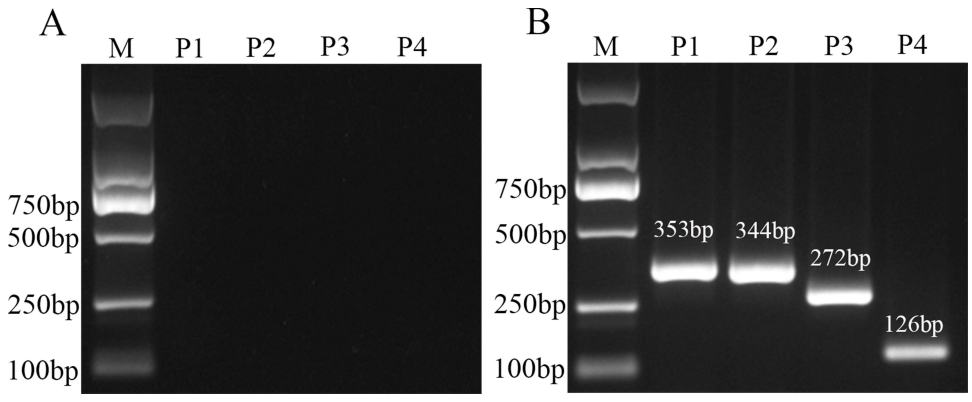

Figure 1 Validation of the primer's own quality and PCR products amplified by 4 pairs of primers with typical strain *M. marinum* DNA. (M) 2000 bp DNA marker, Lanes P1-P4: PCR reaction with *M. marinum* specific primer pairs of 1 (16S rRNA), 2 (rpoB), 3 (hsp20-1), and 4 (hsp20-2) in the absence of *M. marinum* DNA (**A**) and in the presence of *M. marinum* DNA (**B**).

spp., *Baumannii* spp. and *Pseudomonas aeruginosa*. The fungal species included one strain of *Candida albicans* and *Candida tropicalis*, three isolates of *Fonsecaea monophora*, two isolates of *Fonsecaea pedrosoi*, two isolates of *Sporothrix schenckii*, and three isolates of *Sporothrix globosa*.

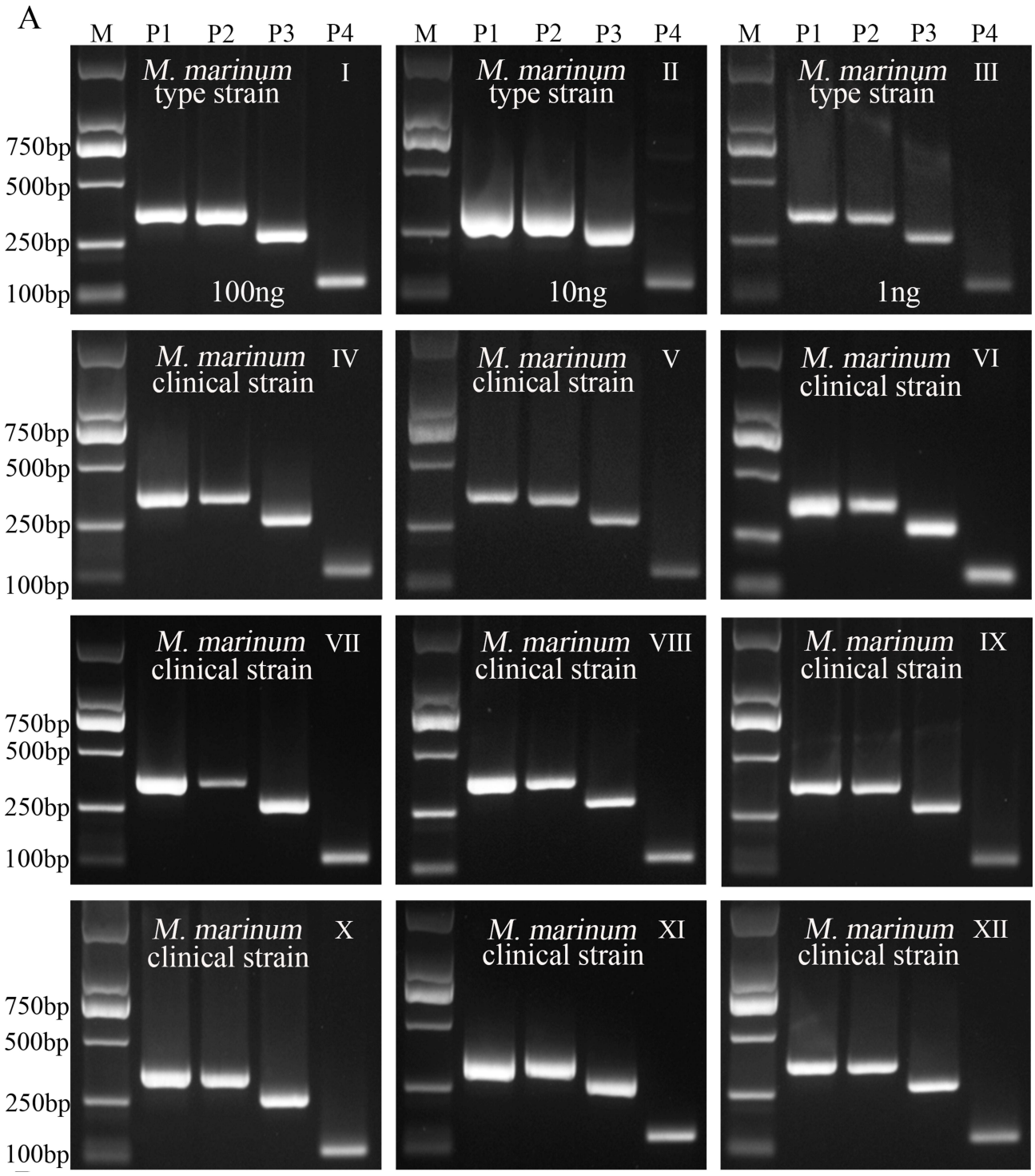

Figure 2 Continued.

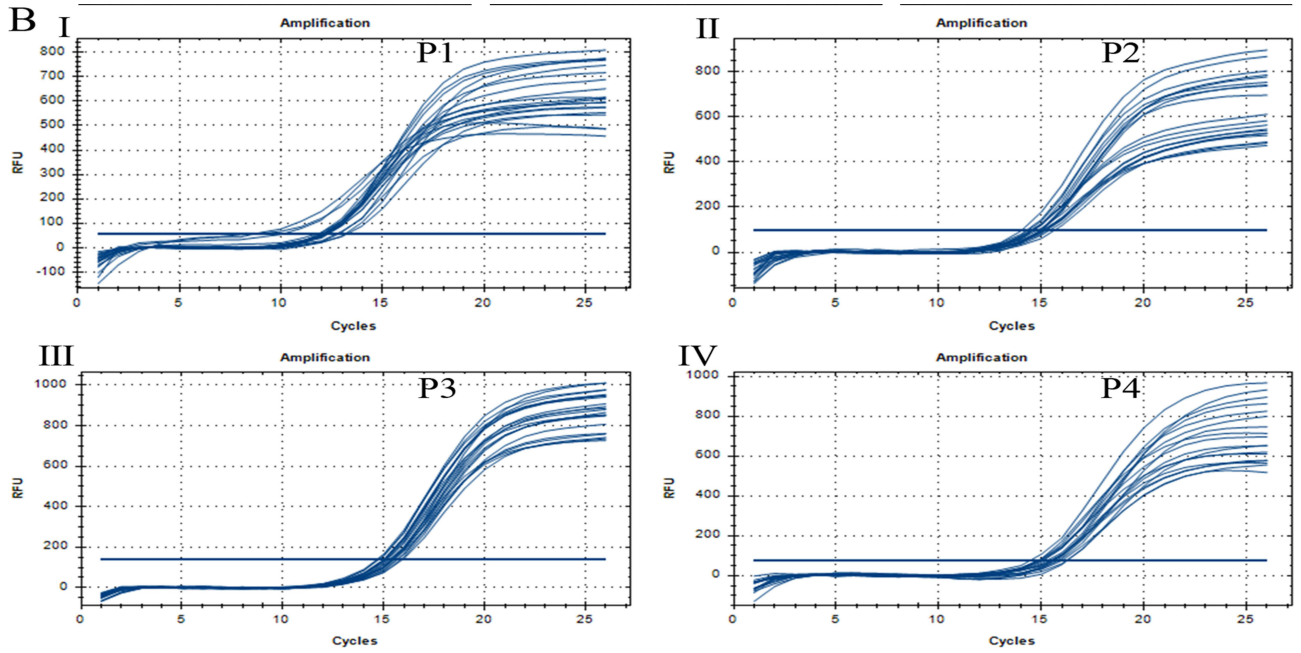

Figure 2 Validation of system sensitivity. (**AI-III**): *(M) marinum* type strain DNA was added at concentrations of 100 ng, 10 ng, and 1 ng in separate PCR assays using four pairs of *M. marinum* primers. (**A IV**-XII): Nine clinical *M. marinum* strain DNAs at a concentration of 100 ng were individually added to each PCR reaction using different sets of four *M. marinum* primers. (M) 2000 bp DNA marker, Lanes labeled as P1, P2, P3, and P4 correspond to the PCR products generated with each pair of primers. (**B** I–IV): Similar amplification curves were observed when using induced typical or clinical *M. marinum* DNAs in the real-time PCR assay with primers 1 (sub-subfigure 2BI), 2 (sub-subfigure 2BII), 3 (sub-subfigure 2BIII), and 4 (sub-subfigure 2BIV).

Our results unequivocally demonstrated that none of the twelve bacterial strains (Figure 4A) or twelve fungal strains (Figure 4B) formed target bands at the expected locations with the 4 pairs of *M. marinum*-specific primers. Meanwhile, the same DNA from each bacterial or fungal species could amplify a respective product with bacterial-specific or fungal-specific primers, as demonstrated by the PCR bands under the "N" line in Figure 4A and B. The absence of amplification curves for each pair of primers was negative with any bacterial DNA (Figure 5A) and any fungal DNA (Figure 5B) in the Real-time PCR assay. Both the PCR and Real-time PCR methods affirm a 100% specificity of our 4-primer pairs system for detecting *M. marinum*.

The Four-Pair Primers PCR is Species-Specific for M. Marinum

We expanded the specificity assessment to include six additional non-tuberculous mycobacteria (NTM), namely *M. chelonae, M. avium, M. intracellulare, M. kansasii, M. scrofulaceum*, and *M. abscessus*. As illustrated in Figure 6, while PCR products, particularly from the 16S rRNA primers, were observed in 4 out of 6 NTM species, and the rpoB product was detected in 5 out of 6 species, the bands corresponding to rpoB did not align with the target bands of *M. marinum* (Figure 1B). Simultaneously, the PCR products for both hsp20-1 and hsp20-2 were negative for all 6 species. Clearly, this 4-primer pair system significantly enhances the identification power at the species level of *Mycobacterium* spp. compared to a single primer set PCR.

Successful Establishment of Infection Model in Mice

To quantitatively assess our 4-pair primers PCR system in infected tissues, we selected five concentrations of *M. marinum* (3×10^8 CFU, 3×10^7 CFU, 3×10^6 CFU, 3×10^5 CFU, 3×10^4 CFU) to inject into the backs of mice. Post-injection during 10–14 days, obvious swelling and nodules were observed on the back (Figure 7A and B). Pathological results revealed evident signs of infected granuloma and a large number of inflammatory cell infiltrations (Figure 7C and D), indicating the successful construction of the mouse model.

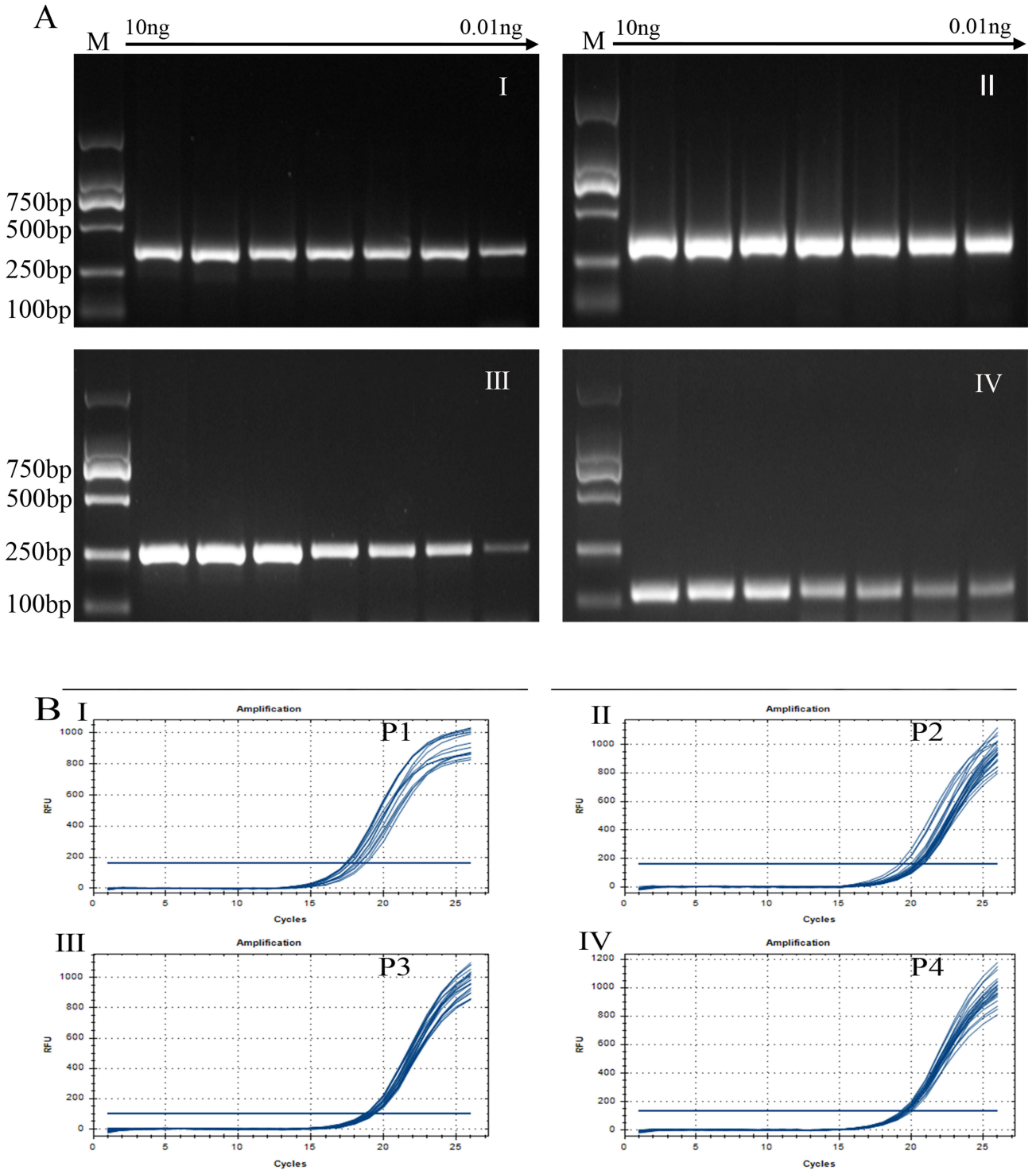

Figure 3 The detection capacity of 4-pair primer system in PCR (**A**) and Real- time PCR (**B**). (**A**). Type *M. marinum* strain DNAs were added at varying amounts, including 10ng, 1ng, 0.08 ng, 0.06ng, 0.04 ng, 0.02ng, to 0.01ng into PCR reaction.(**A** I–IV): PCR amplification revealed the appearance of target bands at expected locations for primers 1 (sub-subfigure 3A (I), 2 (sub-subfigure 3AII), 3 (sub-subfigure 3AIII), and 4 (sub-subfigure 3AIV). (**B** I–IV): Distinct amplification curves for each primer pair, labeled as 1 (sub-subfigure 3BI), 2 (sub-subfigure 3BII), 3 (sub-subfigure 3BIII), and 4 (sub-subfigure 3BIV), were similar across all seven tested concentrations of typical strains using the real-time PCR system.

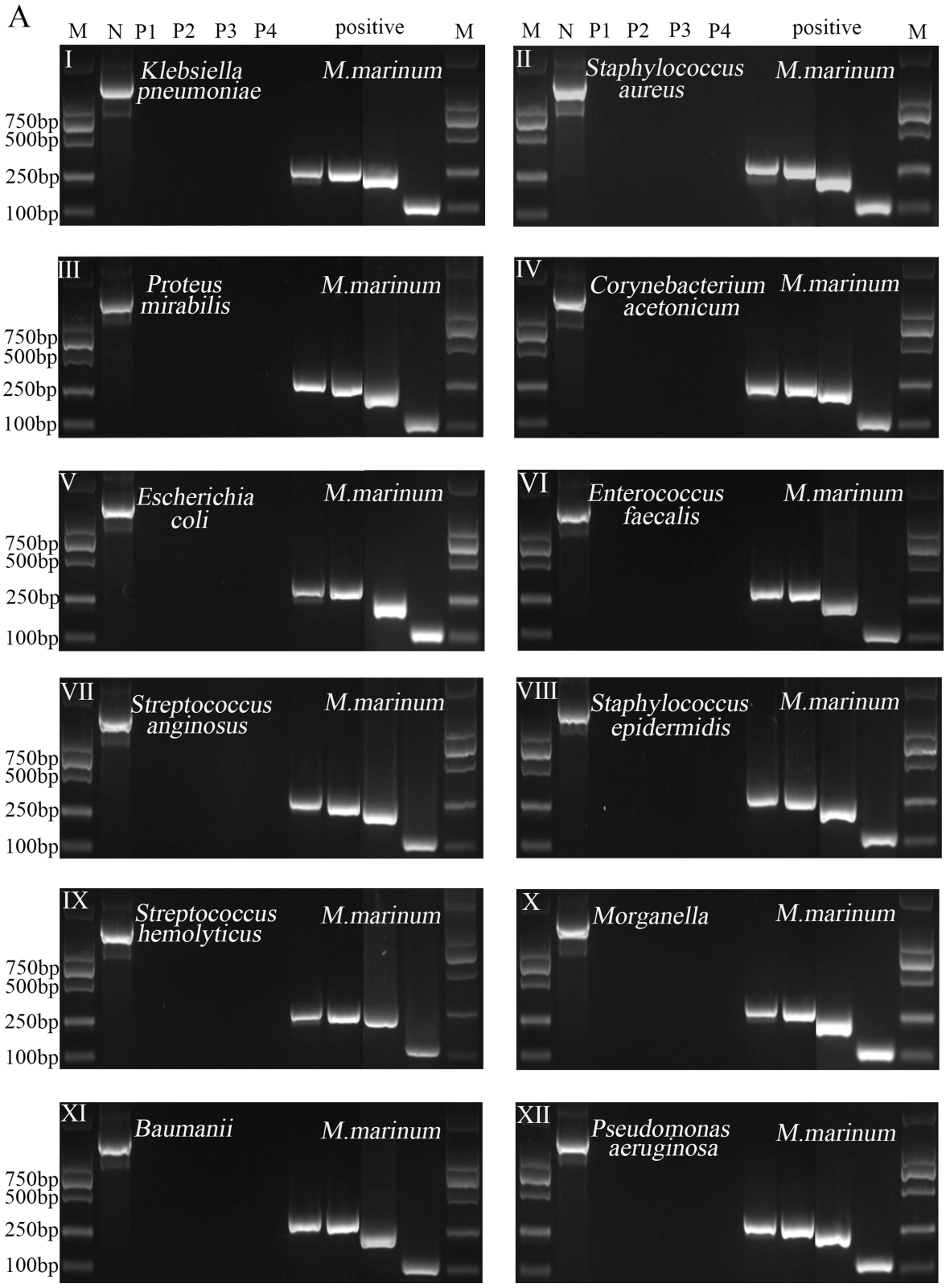

Figure 4 Continued.

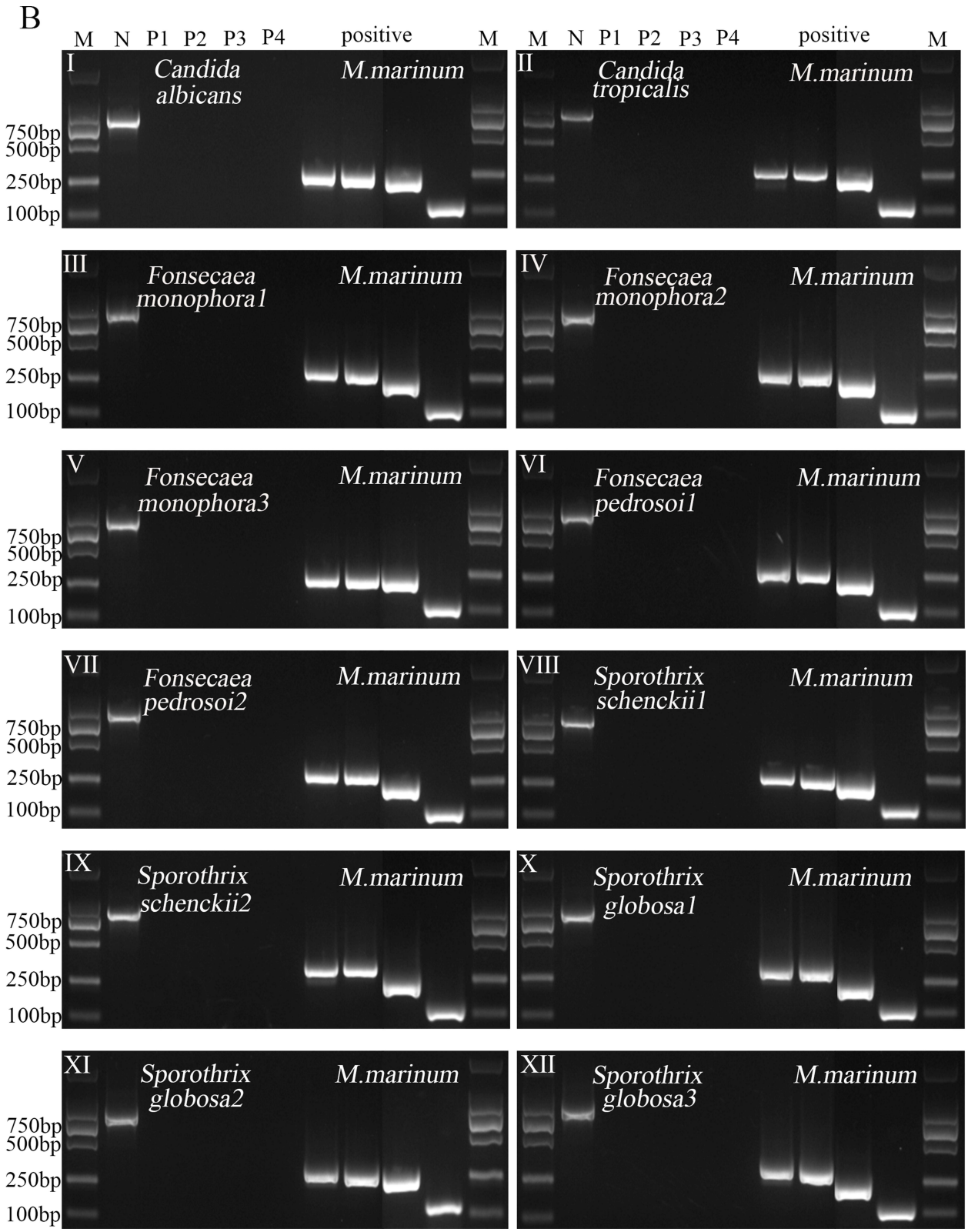

Figure 4 Validation of specificity by PCR system. (**A**I - XII) Negative PCR products with *M. marinum*-specific 4-pair primers in 12 bacterial species, as indicated in each image.The selected bacterial species were *Klebsiella pneumoniae*(I), *Staphylococcus aureus*(II), *Proteus mirabilis*(III), *Corynebacterium acetonicum*(IV), *Escherichia coli*(V), *Enterococcus faecalis*(VI), *Streptococcus anginosus*(VII), *Staphylococcus epidermidis*(VII), *Streptococcus hemolyticus*(IX), *Morganella* (X), *Baumannii* (XI) and *Pseudomonas aeruginosa*(XII). (**B**I - XII) Negative PCR products with 12 fungal species, as indicated, using *M. marinum*-specific 4-pair primers.The fungal species included one strain of *Candida albicans*(I) and *Candida tropicalis*(II), three isolates of *Fonsecaea monophora*(III–V), two isolates of *Fonsecaea pedrosoi*(VI–VII), two isolates of *Sporothrix schenckii*(VII–IX), and three isolates of *Sporothrix globosa*(X–XII). (M) 2000 bp DNA marker; (N) PCR product with universal bacterial or fungal primers; Lanes P1-P4: Bacterial DNA or fungal DNA with each pair of *M. marinum* primers; positive: *(M) marinum* PCR products with 4 pairs of *M. maritimus* primers.

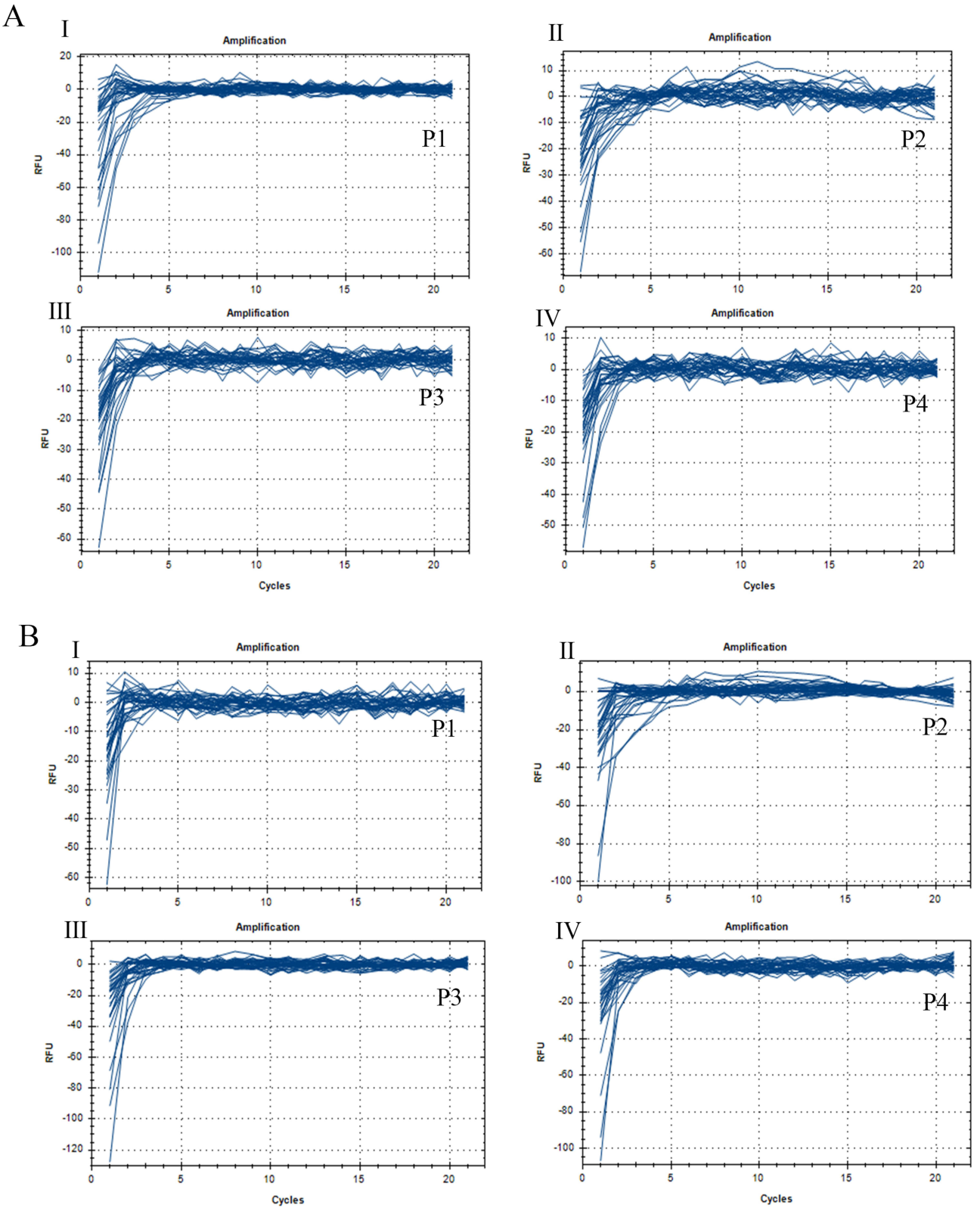

Figure 5 Subfigure A displays that in Real-time PCR assay, no amplification curve was observed with *M. marinum*-specific 4-pair primers in 12 bacterial species.No amplification curve was observed when using 12 bacterial species DNAs in the real-time PCR assay with primers 1 (sub-subfigure (**A**) (I), 2 (sub-subfigure (**A**)II), 3 (sub-subfigure (**A**)III), and 4 (sub-subfigure (**A**)IV) as seen in sub-subfigures AI-IV. Subfigure (**B**) displays that in Real-time PCR assay, no amplification curve was observed with *M. marinum*-specific 4-pair primers in 12 fungal species. No amplification curve was observed when using 12 fungal species DNAs in the real-time PCR assay with primers 1 (sub-subfigure 5B (I), 2 (sub-subfigure 5BII), 3 (sub-subfigure 5B III), and 4 (sub-subfigure 5BIV) as seen in sub-subfigures BI-IV.

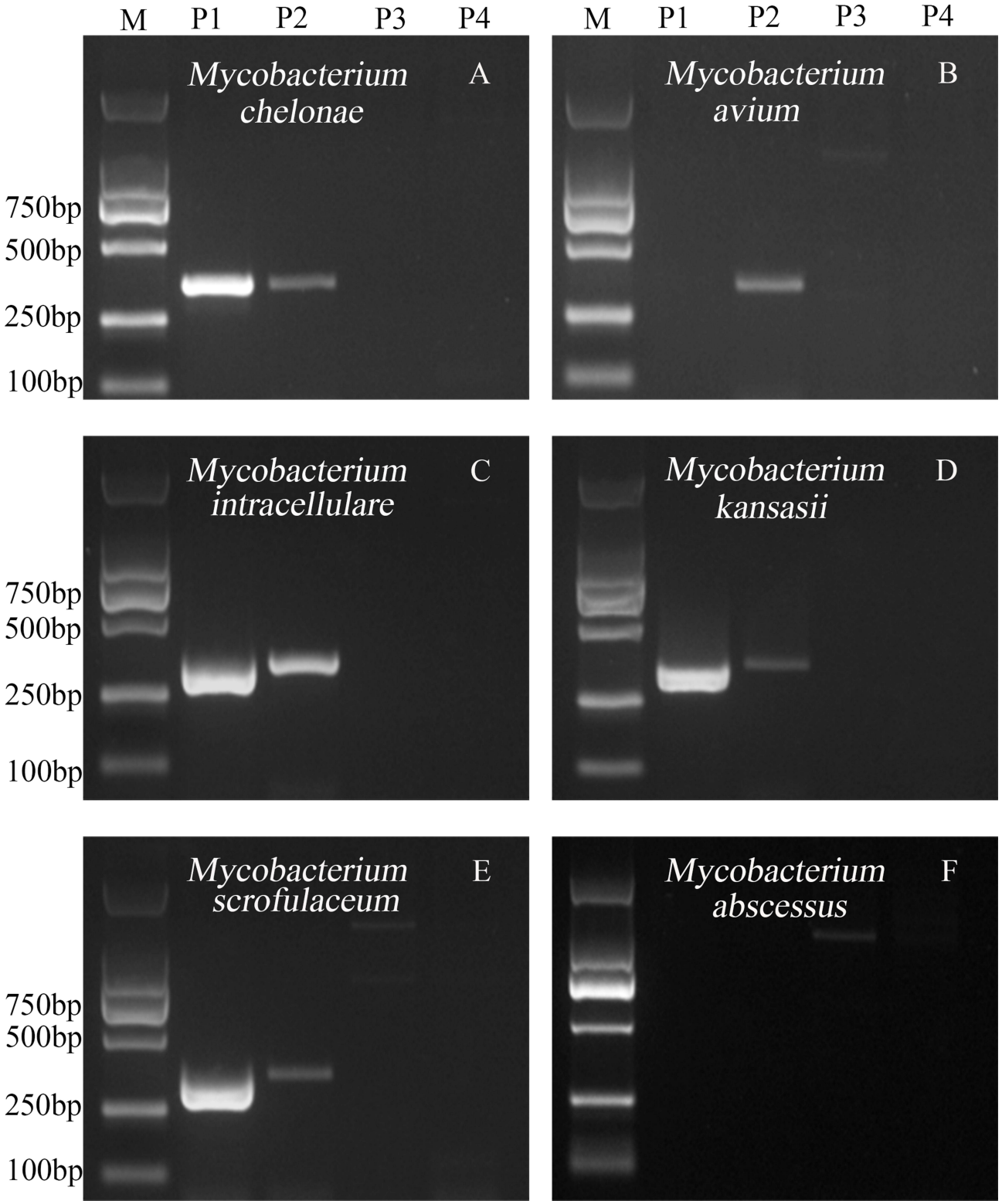

Figure 6 The 4-pair primer PCR method enhances species specificity. DNAs from 6 non-tuberculous mycobacteria showed no typical 4-sized PCR products with *M. marinum*-specific primers. (**A**) *M. chelonae*; (**B**) *M.avium*; (**C**) *M. intracellulare*; (**D**) *M. kansasii*; (**E**) *M. scrofula*; and (**F**) *M. abscessus*. (M) 2000 bp DNA marker; Lanes P1- P4: NTM species DNAs with 4 pairs of *M. maritimus* primers in PCR assay.

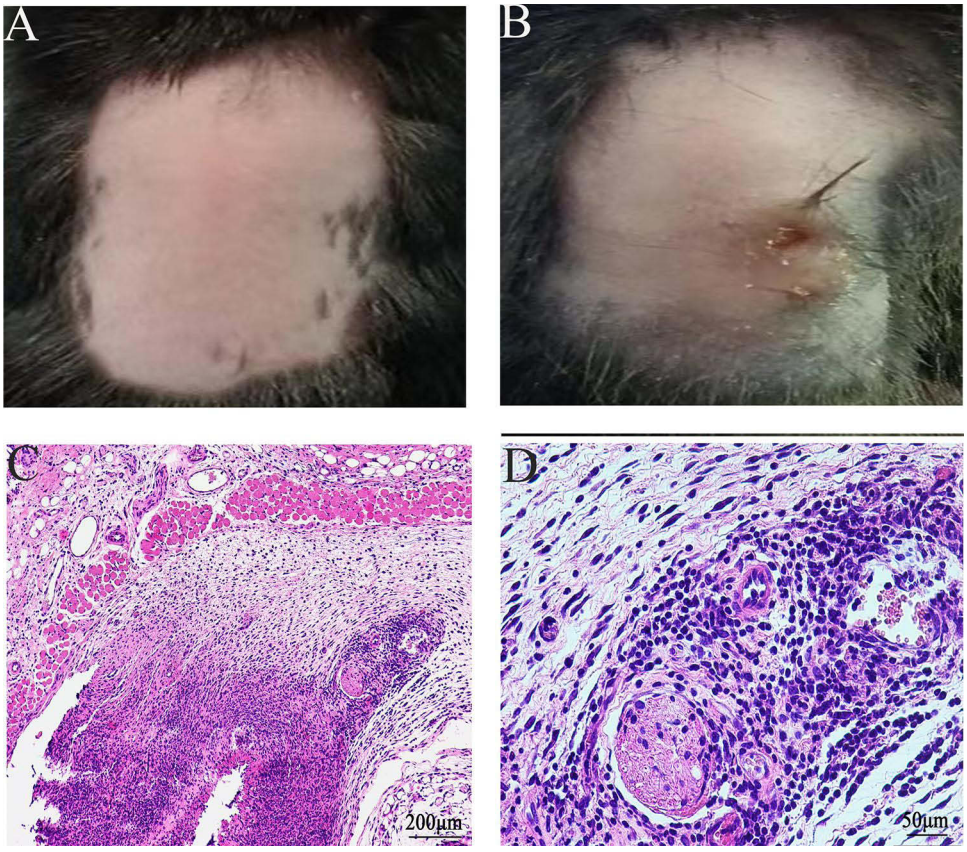

Figure 7 *M. maritimus* infected mouse model. (**A**) Mouse normal skin. (**B**) Infected skin lesions at day 10 post infection in mice. (**C**) Granuloma formation. (**D**) Pathological findings showing typical massive inflammatory cell infiltration.

PCR and Real-Time PCR Validation with Fresh and Paraffin-Embedded Mouse Tissues

By day 14 post-injection, the PCR systems for detecting *M. marinum* were applied to both fresh tissues (Figure 8A) and paraffin-embedded tissues (Figure 8B). In the fresh tissue panel (Figure 8A), DNAs extracted from mice receiving the highest inoculum to the lowest inoculum were further diluted to concentrations of 100 ng, 50 ng, 25 ng, 10 ng, 5 ng, and 1 ng for sensitivity evaluation. Our data demonstrated persistent positive PCR amplifications for all 4 primer sets in mice, even with the lowest inoculum on the skin and highly diluted DNA. However, when compared to the PCR efficiency for fresh tissue, the overall PCR results from paraffin-embedded mouse tissues were less pronounced at each testing concentration (Figure 8B). The compromised PCR results from paraffin-embedded tissues were particularly evident with primer pairs 3 and 4 for hsp20; however, the 16S rRNA and rpoB products remained bright under all testing conditions.

However, the compromised results from paraffin-embedded tissues became less evident when we used Real-time PCR methods. As shown in Figure 9, compared with the fresh tissues (Figure 9A), all the tested DNA concentrations from paraffin-embedded tissues (Figure 9B) produced similar amplification curves despite the variable initial inoculum of *M. marinum*. These in vivo diagnostic results demonstrate that this 4-pair primer system is also applicable in the diagnosis of *M. marinum* infection.

Validation PCR and Real-Time PCR with Paraffin-Embedded Tissue Samples Obtained from Clinically Infected Patients

All four patients exhibited typical nodular skin manifestations on their hands, as depicted in Figure 10A. The paraffin-embedded skin samples were obtained as part of the biopsy for pathological diagnosis. Utilizing the PCR system, positive detection of *M. marinum* (Figure 10B) was notably evident with primer pairs 1, 2, and 4 (hsp20-2), although less pronounced with primer pair 3 (hsp-1), across all four clinical samples. The detection method exhibited 100% validity in

clinical paraffin-embedded tissue. Using Real-time PCR methods, as illustrated in Figure 10C, the tested DNAs from paraffin-embedded tissues generated similar amplification curves. These clinical findings once again underscored the applicability of this 4-pair primer system in diagnosing *M. marinum* infection.

Discussion

M. marinum, a slow-growing atypical mycobacterium, initially associated with aquaculture animals and fish industry,[17,18] has recently attracted attention from clinical dermatologists due to an increase in *M. marinum* skin infection.[19–21] Except for its water contact medical history, the absence of typical clinical manifestations, coupled challenges in laboratory examination and radiologic features, often leads to misdiagnosis of *M. marinum* skin infection as fungal infections.[22,23] The gold-standard culture method, predominantly used in clinical settings, requires an incubation period of 2–8 weeks for distinct colonies to become visible to the naked eye, even though positivity rate is low.[24] Consequently, the delay in definitive diagnosis of *M. marinum* infection significantly impacts the therapeutic outcomes.

Histopathologic and immunologic techniques have been integral in diagnosing *M. marinum* infections.[25] These methods include anti-acid staining, immunofluorescence, and immune in situ hybridization to detect the organism within infected tissues. While the positive rate of anti-acid staining is generally low,[26] as confirmed by numerous studies, more sensitive techniques like immunofluorescence staining or immune in situ hybridization also rely on the organism's abundance in the tissues. The accuracy of these methods remains a concern until specific immunomarkers aiding

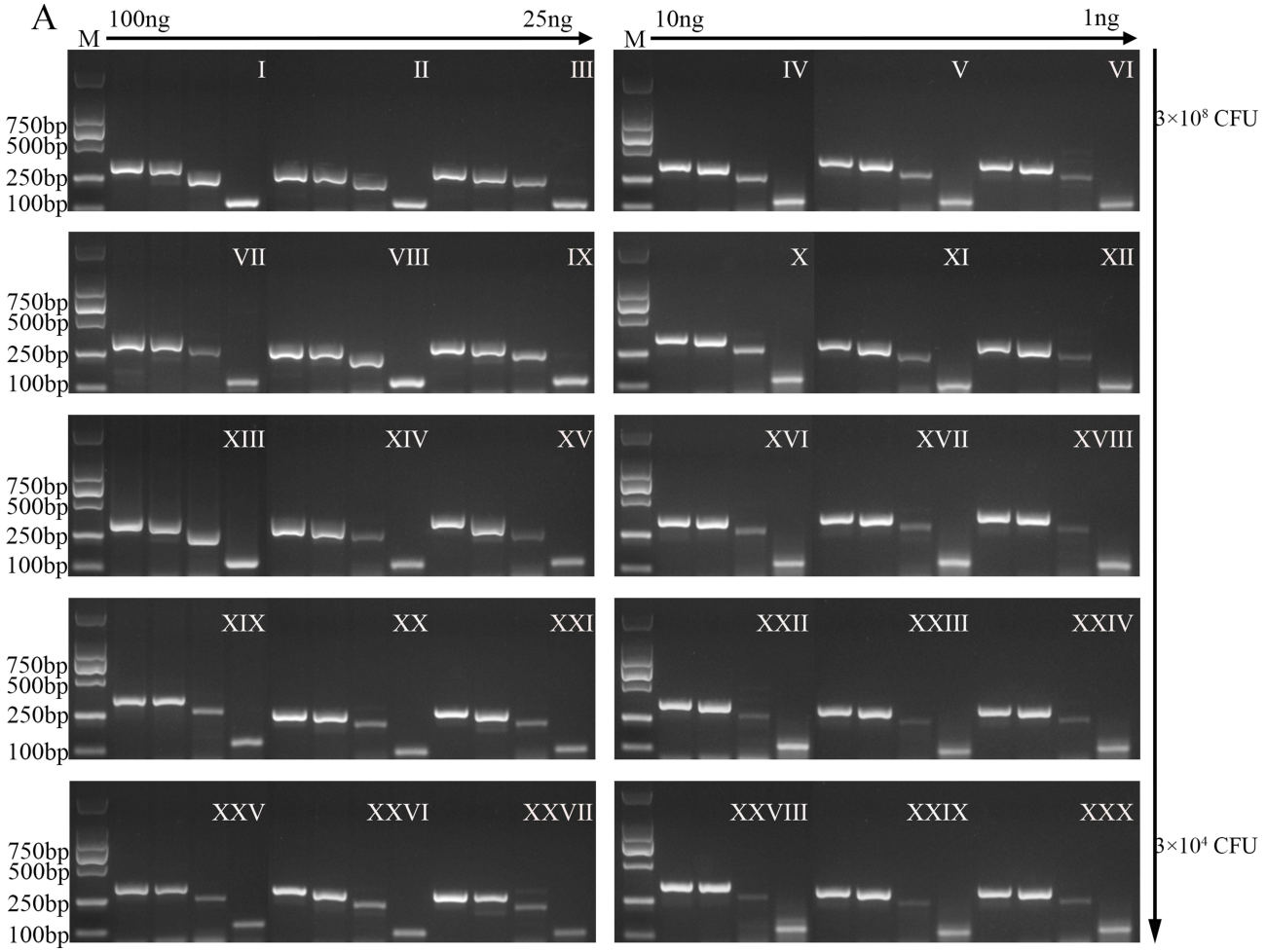

Figure 8 Continued.

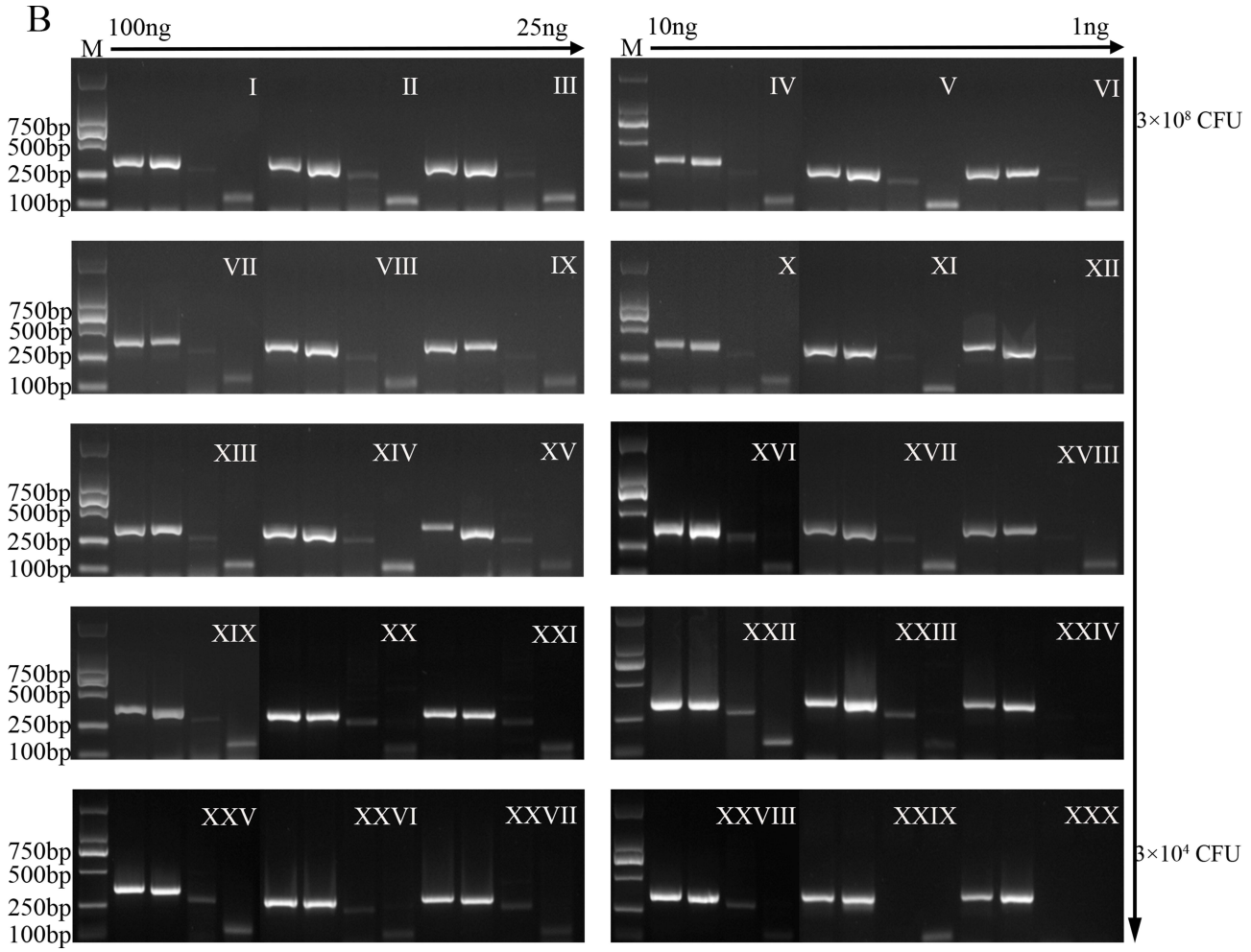

Figure 8 The DNA extracted from fresh tissues (subfigure (**A**) displayed more pronounced results compared to the paraffin-embedded tissues (subfigure (**B**) in PCR assay with *M. marinum*-specific 4-pair primers. Subfigure (**A**) displays that the DNA extracted from fresh tissues extracted from mice receiving the highest inoculum (3×10^8 CFU) to the lowest inoculum (3×10^4 CFU) was added at concentrations of 100 ng, 50 ng, 25 ng, 10 ng, 5 ng, and 1 ng in separate PCR assays using four pairs of *M. marinum* primers as seen in sub-subfigures AI-XXX. Subfigure (**B**) displays that the DNA extracted from paraffin-embedded tissues extracted from mice receiving the highest inoculum (3×10^8 CFU) to the lowest inoculum (3×10^4 CFU) was added at concentrations of 100 ng, 50 ng, 25 ng, 10 ng, 5 ng, and 1 ng in separate PCR assays using four pairs of *M. marinum* primers as seen in sub-subfigures BI-XXX.

M. marinum diagnosis are identified. Enhanced understanding of the immunopathological basis for tissue infiltration in *M. marinum* infection may hold promise for optimizing these immunopathologic diagnostic tools for clinical use.

PCR-based technology has been extensively investigated for diagnosing infectious agents, including *M. marinum*. However, earlier developments primarily relied on amplification detections based on single genes or sequences,[27,28] resulting in poor sensitivity and specificity. Specificity is particularly concerning in this diagnostic procedure, as a single gene may exhibit high similarity among atypical *Mycobacterium* species, as illustrated by the 16S rRNA results in this study (Figure 6). The limitation of single-gene detection is evident in the presence of unavoidable false-positive results. In this study, we refined a 4-pair primers system, successfully distinguishing *M. marinum* from other bacteria and fungi, and importantly, from six other species of *Mycobacterium* organisms.

To assess the feasibility of this diagnostic procedure in infection sites, we established a mouse infection model and examined the feasibility of DNA extraction and *M. marinum* detection in both fresh and paraffin-embedded infected tissues. The selection of these two types of specimens was based on the prevalent availability of fresh tissue or retrospective paraffin tissue samples for diagnosing *M. marinum*.[29] In this study, we enhanced a nucleic acid extraction method to accommodate small sample volumes by extending the lysis period for *M. marinum*, ensuring efficient DNA

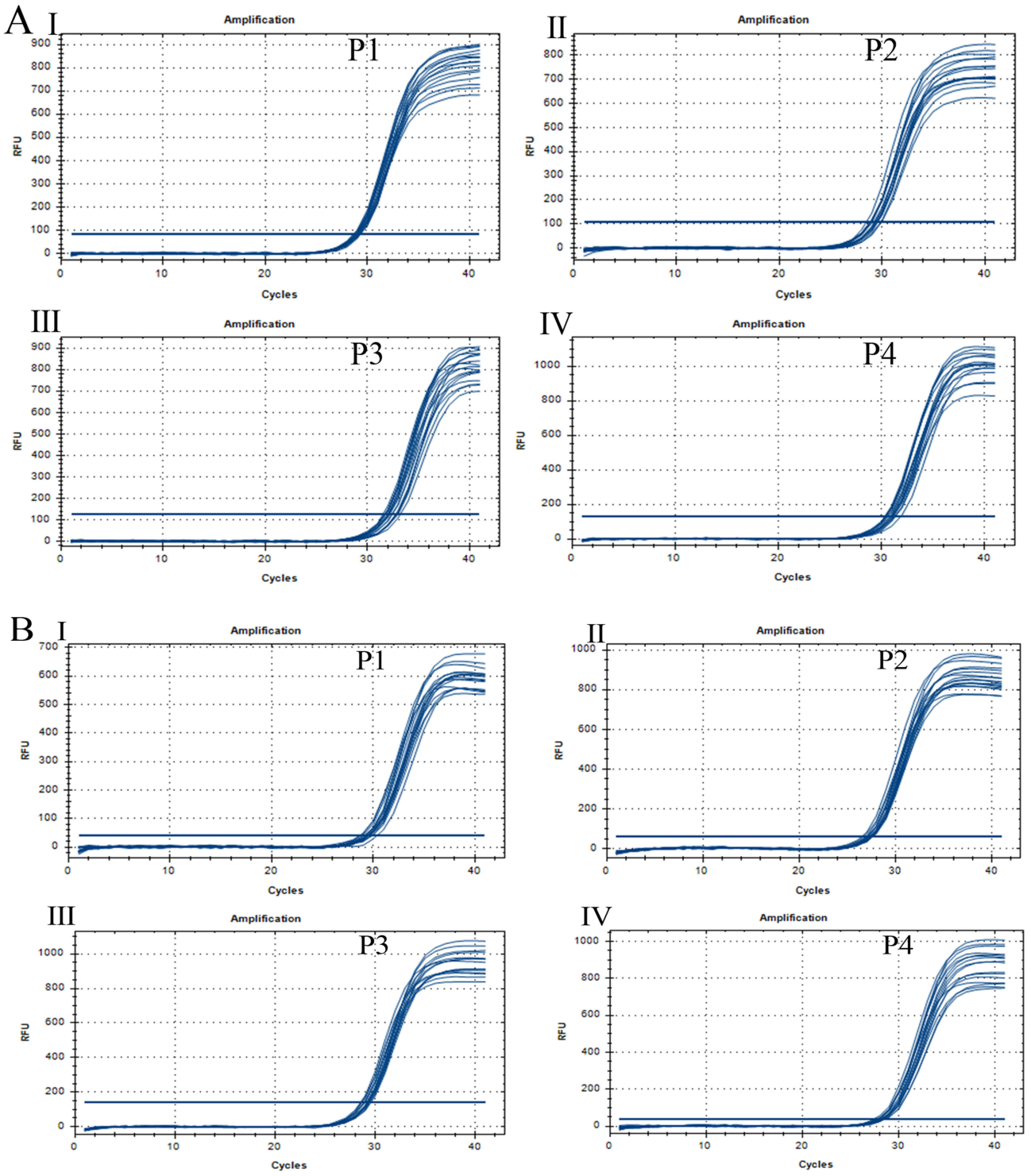

Figure 9 Real-time PCR assay with M. marinum-specific 4-pair primers in fresh tissues of infected mice (subfigure (**A**) and in paraffin-embedded tissues (subfigure (**B**) shows equal efficiency of both tissue samples. Subfigure (**A**) displays that similar amplification curves were observed when using fresh tissues of infected mice DNAs in the real-time PCR assay with primers 1 (sub-subfigure 9A (I), 2 (sub-subfigure 9AII), 3 (sub-subfigure 9A III), and 4 (sub-subfigure 9A IV) as seen in sub-subfigures AI-IV. Subfigure (**B**) displays that similar amplification curves were observed when using paraffin-embedded tissues of infected mice DNAs in the real-time PCR assay with primers 1 (sub-subfigure 9B (I), 2 (sub-subfigure 9BII), 3 (sub-subfigure 9B III), and 4 (sub-subfigure 9B IV) as seen in sub-subfigures BI-IV.

release. Despite improvements in DNA extraction, the PCR-based detection sensitivity of paraffin-embedded tissues was still lower compared to fresh tissues. This disparity is attributed to the limited sample size of paraffin-embedded tissues and nucleic acid damage incurred during fixation.

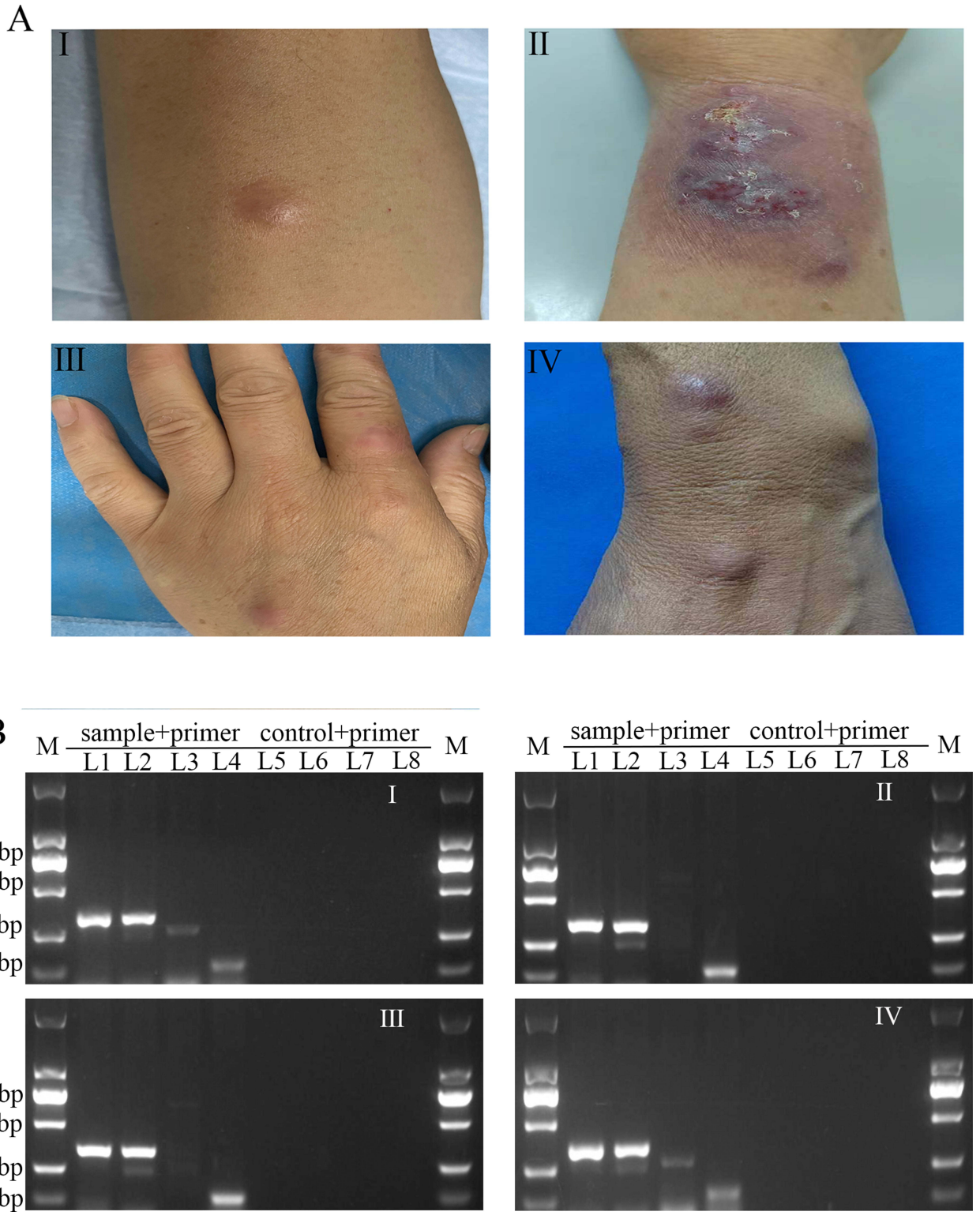

Figure 10 Continued.

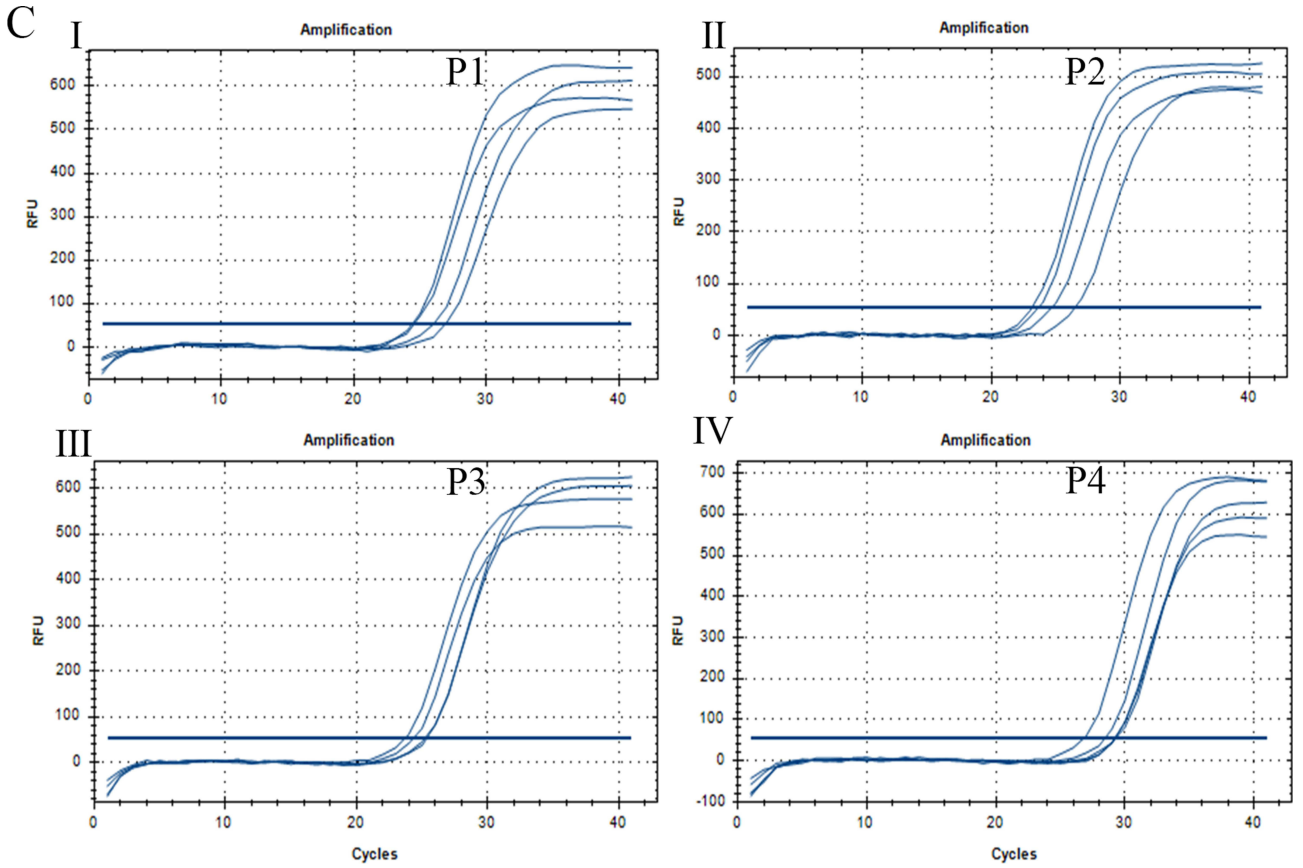

Figure 10 (**A** I–IV) Four clinical patients demonstrated manifestations of significant infected skin lesions. (**B** I–IV): PCR amplification revealed the appearance of target bands at expected locations with *M. marinum*-specific 4-pair primers in 4 clinical skin tissues. (M) 2000 bp DNA marker, Lanes L1-L4: PCR reaction with *M. marinum* specific primer pairs of 1 (16S rRNA), 2 (rpoB), 3 (hsp20-1), and 4 (hsp20-2) in the presence of DNA from clinical skin tissues. Lanes L5-L8: PCR reaction with *M. marinum* specific primer pairs of 1 (16S rRNA), 2 (rpoB), 3 (hsp20-1), and 4 (hsp20-2) in the absence of *M. marinum* DNA. (**C**) Real-time PCR assay with *M. marinum*-specific 4-pair primers in paraffin-embedded tissues displays the amplification curves in 4 paraffin-embedded tissues.(**C** I–IV): Similar amplification curves were observed when using paraffin-embedded tissues DNAs in the real-time PCR assay with primers 1 (sub-subfigure 10C (I), 2 (sub-subfigure 10CII), 3 (sub-subfigure 10C III), and 4 (sub-subfigure 10C IV).

Next-generation sequencing (NGS) technology has revolutionized pathogen detection, particularly in clinical samples, owing to its rapidity, accuracy, and independence from microbial culture.[30] This high-throughput nucleic acid technique is engineered to sequence entire genomes or specific regions of DNA or RNA, enabling rapid pathogen identification. Compared to traditional microbial diagnostic methods like tissue anti-acid staining and tissue culture, NGS offers superior diagnostic efficacy.[31,32] However, it also presents some drawbacks, such as high cost and complexity procedure, which hinder its widespread adoption in clinical diagnosis within a short timeframe.

The detection system developed in this study offers several advantages. It takes approximately 4 hours from obtaining nucleic acid extraction to completing the test, with a simple operational procedure. Additionally, the instrumentation used in the system is cost-effective, making the test more rapid and economically viable compared to second or third-generation sequencing methods. These factors facilitate easier promotion of the test to grassroots levels. Moreover, its suitability for wider-scale epidemiological studies on *M. marinum* samples enhances its utility in research and public health initiatives.

The primary limitation of this study is the lack of validation of the assay's feasibility on a larger scale with clinical samples. Future research will focus on validating the assay using both fresh tissues and paraffin-embedded tissues. Additionally, the current system employs a dye-based method for Real-time PCR. Enhancements in sensitivity and stability can be achieved by designing fluorescent probes for the amplified regions and potentially integrating droplet digital PCR (ddPCR) technology into the system in future iterations.

Conclusion

In our study, we explored both PCR and real-time PCR with 4-primer sets to identify *M. marinum* in vitro, in fresh and paraffin-embedded skin tissues from infected mice, and in four skin samples from infected patients. By referencing negative results from other bacterial or fungal species in vitro and validating in vivo infected tissue, we have initially established a sensitive and highly specific rapid detection system for *M. marinum*. This system shows promise for rapidly detecting M. *marinum* in both fresh and paraffin-embedded tissues. Our findings suggest that this method can significantly improve the speed and accuracy of *M. marinum* diagnosis, potentially leading to better patient outcomes through timely and precise treatment interventions. We look forward to further validating this method with a larger sample size and a wider variety of clinical specimens in future studies.

Data Sharing Statement

All data generated or analyzed during this study are included in this published article.

Ethics Approval and Informed Consent

This study was approved by the Institutional Research and Ethics Committee of Jining No. 1 People's Hospital (KYLL-202309-162) and was approved by the Inspection and Approval of animal ethical and Welfare in Jining NO.1 People's Hospital (JNRM-2023-DW-104). The name of the guidelines followed for the welfare of the laboratory animals is Laboratory animals-General code of animal welfare.All patients provided their written informed consent to participate in this study. The study was carried out in accordance with the principles of the Declaration of Helsinki. The first author vouches for the completeness and accuracy of the data and for the adherence of the study to the protocol.

Acknowledgments

We are grateful to all the authors for their contributions to this study.

Funding

This work was supported by grants from the National Nature Science Foundation of China (NM 82272358), the Key Research and Development Plan of Jining (NM 2021YXNS121), and the Tra-ditional Chinese Medicine Science and Technology Program of Shandong Province (NM 2021M080).

Disclosure

The authors declare that they have no competing interests in this work.

References

1. Bouceiro-Mendes R, Ortins-Pina A, Fraga A, et al. Mycobacterium marinum lymphocutaneous infection. *Dermatol Online J*. 2019;25(2):13030/qt5bb78905. doi:10.5070/D3252042893
2. Tebruegge M, Curtis N. Mycobacterium marinum infection. *Adv Exp Med Biol*. 2011;719:201–210.
3. Bouricha M, Castan B, Duchene-Parisi E, et al. Mycobacterium marinum infection following contact with reptiles: vivarium granuloma. *Int J Infect Dis*. 2014;21:17–18. doi:10.1016/j.ijid.2013.11.020
4. Tomas X, Pedrosa M, Soriano A, et al. Rare diagnosis of nodular lymphangitis caused by Mycobacterium marinum: MDCT imaging findings. *Acta Radiol Short Rep*. 2014;3(2):2047981614523172. doi:10.1177/2047981614523172
5. Oh TH, Kim UJ, Kang SJ, et al. Disseminated invasive mycobacterium marinum infection involving the lung of a patient with diabetes mellitus. *Infect Chemother*. 2018;50(1):59–64. doi:10.3947/ic.2018.50.1.59
6. El Amrani MH, Adoui M, Patey O, et al. Upper extremity Mycobacterium marinum infection. *Orthop Traumatol Surg Res*. 2010;96(6):706–711. doi:10.1016/j.otsr.2010.02.016
7. Guarneri C, Cannavò SP. 'Fish-tank' granuloma: a diagnostic dilemma. *Intern Med J*. 2009;39(5):338–339. doi:10.1111/j.1445-5994.2009.01923.x
8. Hashish E, Merwad A, Elgaml S, et al. Mycobacterium marinum infection in fish and man: epidemiology, pathophysiology and management; a review. *Vet Q*. 2018;38(1):35–46. doi:10.1080/01652176.2018.1447171
9. Eberst E, Dereure O, Guillot B, et al. Epidemiological, clinical, and therapeutic pattern of Mycobacterium marinum infection: a retrospective series of 35 cases from southern France. *J Am Acad Dermatol*. 2012;66(1):e15–6. doi:10.1016/j.jaad.2011.01.024
10. Chen S, Liu Z, Xia X. Scubcutaneous Mycobacterium marinum infection misdiagnosed as sporotrichosis: a case report. *Medicine (Baltimore)*. 2022;101(49):e32220. doi:10.1097/MD.0000000000032220
11. Tsiolakkis G, Liontos A, Filippas-Ntekouan S, et al. Mycobacterium marinum: a case-based narrative review of diagnosis and management. *Microorganisms*. 2023;11(7):1799. doi:10.3390/microorganisms11071799

12. Strobel K, Sickenberger C, Schoen C, et al. Diagnosis and therapy of Mycobacterium marinum: a single-center 21-year retrospective analysis. *J Dtsch Dermatol Ges*. 2022;20(9):1211–1218.
13. Schaefer WB, Davis CL. A bacteriologic and histopathologic study of skin granuloma due to Mycobacterium balnei. *Am Rev Respir Dis*. 1961;84:837–844. doi:10.1164/arrd.1961.84.6.837
14. Xing F, Lo SKF, Ma Y, et al. IRapid diagnosis of mycobacterium marinum infection by next-generation sequencing: a case report. *Front Med Lausanne*. 2022;9:824122. doi:10.3389/fmed.2022.824122
15. Avaniss-Aghajani E, Jones K, Holtzman A, et al. Molecular technique for rapid identification of mycobacteria. *J Clin Microbiol*. 1996;34 (1):98–102. doi:10.1128/jcm.34.1.98-102.1996
16. Talaat AM, Reimschuessel R, Trucksis M. Identification of mycobacteria infecting fish to the species level using polymerase chain reaction and restriction enzyme analysis. *Vet Microbiol*. 1997;58(2–4):229–237. doi:10.1016/S0378-1135(97)00120-X
17. Holden IK, Kehrer M, Andersen AB, et al. Mycobacterium marinum infections in Denmark from 2004 to 2017: a retrospective study of incidence, patient characteristics, treatment regimens and outcome. *Sci Rep*. 2018;8(1):6738. doi:10.1038/s41598-018-24702-7
18. Johnson MG, Stout JE. Twenty-eight cases of Mycobacterium marinum infection: retrospective case series and literature review. *Infection*. 2015;43 (6):655–662. doi:10.1007/s15010-015-0776-8
19. Mei Y, Zhang W, Shi Y, et al. Cutaneous tuberculosis and nontuberculous mycobacterial infections at a national specialized hospital in China. *Acta Derm Venereol*. 2019;99(11):997–1003. doi:10.2340/00015555-3283
20. Veraldi S, Pontini P, Nazzaro G. Amputation of a finger in a patient with multidrug-resistant Mycobacterium marinum skin infection. *Infect Drug Resist*. 2018;11:2069–2071. doi:10.2147/IDR.S179815
21. Chen X, Zhang D, Wang T, et al. Ruxolitinib treatment during myelofibrosis leads to cutaneous mycobacterium marinum infection: a case report. *Clin Cosmet Invest Dermatol*. 2023;16:1499–1503. doi:10.2147/CCID.S413592
22. Khadka DK, Acharya R, Agrawal S. Sporotrichoid lymphocutaneous pattern in a fish-merchant under immunosuppressant medications: clues to differential diagnoses. *Clin Case Rep*. 2022;10(12):e6708. doi:10.1002/ccr3.6708
23. Trčko K, Plaznik J, Miljković J. Mycobacterium marinum hand infection masquerading as tinea manuum: a case report and literature review. *Acta Dermatovenerol Alp Pannonica Adriat*. 2021;30(2):91–93.
24. Aubry A, Mougari F, Reibel F, et al. Mycobacterium marinum. *Microbiol Spectr*. 2017;5(2). doi:10.1128/microbiolspec.TNMI7-0038-2016
25. Sia TY, Taimur S, Blau DM, et al. Clinical and pathological evaluation of mycobacterium marinum group skin infections associated with fish markets in New York City. *Clin Infect Dis*. 2016;62(5):590–595. doi:10.1093/cid/civ937
26. Spiliopoulou A, Kyriakou G, Georgiou S, et al. Acid-fast bacteria as causative agents of skin and soft tissue infections: case presentations and literature review. *Rev Inst Med Trop Sao Paulo*. 2023. doi:10.1590/s1678-9946202365029
27. Feng Y, Wang M, Jiang H, et al. Comparative evaluation of LAMP and nested PCR for the rapid diagnosis of mycobacterium marinum infection. *Infect Drug Resist*. 2023;16:1601–1609. doi:10.2147/IDR.S404929
28. Liu LL, Chen SJ, Long H, et al. [Establishment of multiplex PCR method for rapid detection of nontuberculous mycobacteriums infection in the hand]. *Zhonghua Yi Xue Za Zhi*. 2016;96(14):1116–1119. Chinese. doi:10.3760/cma.j.issn.0376-2491.2016.14.011
29. Bao JR, Clark RB, Master RN, et al. Acid-fast bacterium detection and identification from paraffin-embedded tissues using a PCR-pyrosequencing method. *J Clin Pathol*. 2018;71(2):148–153. doi:10.1136/jclinpath-2016-204128
30. Griffith DE, Aksamit T, Brown-Elliott BA, et al. An official ATS/IDSA statement: diagnosis, treatment, and prevention of nontuberculous mycobacterial diseases. *Am J Respir Crit Care Med*. 2007;175(4):367–416. doi:10.1164/rccm.200604-571ST
31. Gu A, Jiang J, Ma F, et al. Metagenomic next-generation sequencing for the aetiological diagnosis of Mycobacterium marinum infections: a pilot study. *Indian J Dermatol Venereol Leprol*. 2023;89(5):745–748. doi:10.25259/IJDVL_768_2022
32. Tarashi S, Sakhaee F, Masoumi M, et al. Molecular epidemiology of nontuberculous mycobacteria isolated from tuberculosis-suspected patients. *AMB Express*. 2023;13(1):49. doi:10.1186/s13568-023-01557-4